International Journal of Solids and Structures 50 (2013) 1108–1119

Contents lists available at SciVerse ScienceDirect

International Journal of Solids and Structures

journal homepage: www.elsevier.com/locate/ijsolstr

Thermo-mechanical contact behavior of a finite graded layer under a sliding punch with heat generation

Peijian Chen, Shaohua Chen *

LNM, Institute of Mechanics, Chinese Academy of Sciences, Beijing 100190, China

ARTICLE INFO

Article history:
Received 23 September 2011
Received in revised form 16 December 2012
Available online 27 December 2012

Keywords:
Contact mechanics
Finite graded layer
Flat punch
Thermal contact
Wear resistance

ABSTRACT

The problem of a rigid punch contacting with a finite graded layer on a rigid substrate is investigated within the framework of steady-state plane strain thermoelasticity, in which heat generated by contact friction is considered with a constant friction coefficient and inertia effects are neglected. The material properties of the graded layer vary according to an exponential function in the thickness direction. Fourier integral transform method and transform matrix approach are employed to reduce the current thermocontact problem to the second kind of Cauchy-type singular integral equation. Distributions of the contact pressure and the in-plane stress under the prescribed thermoelastic environment with different parameter combinations, including ratio of shear moduli, relative sliding speed, friction coefficient and thermal parameters are obtained and analyzed, as well as the stress singularity and the stress intensity factors near the contact edges. The results should be helpful for the design of surfaces with strong wear resistance and novel graded materials for real applications.

1. Introduction

Functionally graded material (FGM) has been an important smart one to be widely used in various modern engineering practices as an alternative to the conventional homogeneous material, which can be synthesised by at least two kinds of material particles with volume fractions varying in a spatial direction. Used as a coating layer or an interfacial material, it tends to reduce mismatching stresses, increase the bonding strength, improve surface properties and provide protection against adverse thermal or chemical environments (Suresh and Mortensen, 1998). Many of the present and potential applications of FGM involve surface or interface contact, in which loads transfer between or among different solids, generally in the presence of friction. One of the typical applications of FGM is used as cylinder linings, brake discs and other automotive components for the purpose of improving the wear resistance. Another area of the potential applications of FGM involving contact mechanics is in the field of abradable seal design in stationary gas turbines (Guler and Erdogan, 2007).

In the past few years, many studies indicate that controlled gradients in mechanical properties of compositions and structures offer unprecedented opportunities for the design of surfaces with improving resistance to contact deformation and damage (Pender et al., 2001a,b; Suresh et al., 1999; Suresh, 2001). Suresh et al. (1997a,b), Jorgensen et al. (1998) and Krumova et al. (2001) studied theoretically and experimentally the indentation problems to characterize the local properties of FGMs. Giannakopoulos and Suresh (1997a,b) considered the axisymmetric problems of a functionally graded half-space subjected to a concentrated force or an indenter with flat, spherical or conical indentation tip. Their results demonstrated that proper gradient variation of the elastic modulus could greatly change the stress distributions around the indenter and alleviate the Hertzian cracking at the contact edges. Sliding contact problems coupled with a crack in a functionally graded coating has been studied by Dag and Erdogan (2002) and Guler and Erdogan (2004), in which the graded material property varies exponentially. Wang and his co-authors analyzed systematically the plane (Ke and Wang, 2006, 2007), axisymmetric (Liu and Wang, 2008) and fretting (Ke and Wang, 2008, 2010) contact problems of FGMs with a linear multilayered model. Receding contact between a functionally graded coating and a homogeneous substrate as well as the partial slip contact problem were investigated by El-Borgi and his co-authors (El-Borgi et al., 2006; Elloumi et al., 2010; Rhimi et al., 2009). Choi (2009) analyzed the plane contact model of a functionally graded elastic layer loaded by a sliding flat punch, and the corresponding one coupled with a crack was studied by Choi and Paulino (2010).

All the above theoretical models about graded materials belong to the Hertz-type contact. As for adhesive contact models of graded materials, several typical works should be mentioned. The plane strain adhesive contact model of a rigid cylinder on an elastic half-space was studied by Giannakopoulos and Pallot (2000), in which the elastic modulus of the half space varies with the depth

* Corresponding author. Tel.: +86 10 82543960; fax: +86 10 82543977.
E-mail address: chenshaohua72@hotmail.com (S. Chen).

0020-7683/$ - see front matter © 2012 Elsevier Ltd. All rights reserved.
http://dx.doi.org/10.1016/j.ijsolstr.2012.12.007

according to a power law. Chen et al. (2009a) further discussed the corresponding plane strain model and gave a very simple closed-form analytical solution for the model of a rigid sphere contacting with a graded elastic half-space (Chen et al., 2009b). The contact problem with a flaw tolerant adhesive interface was also investigated by Chen and Chen (2010). Recently, the corresponding non-slipping plane strain and axis-symmetric adhesive contact models were further analyzed by Jin and Guo (2010) and Guo et al. (2011).

It should be noted that no thermal effects are considered in the above literatures. However, heat may be generated due to frictional tractions in a moving contact problem and elevated temperature induced by the sliding contact may considerably influence the mechanical performance of FGM or FGM coated structures (Barber, 1976; Barber and Comninou, 1989; Choi and Paulino, 2008; Zhou and Lee, 2011). For homogeneous materials, heat effect in contact problems has been extensively discussed (Barber, 1976; Ciavarella and Barber, 2005; Hills and Barber, 1985, 1986; Hills et al., 1993; Pauk, 1994, 1999; Pauk and Wozniak, 2003, 1999; Yevtushenko and Kulchytskyzhyhailo, 1995). However, for graded materials, very limited literatures consider the thermoelastic contact. Choi and Paulino (2008) analyzed the thermoelastic contact of a flat punch sliding over a sandwich structure, i.e., a homogeneous coating on a homogeneous half space with a graded interlayer. Barik et al. (2008) considered a stationary plane contact model between a functionally graded heat conducting punch and a rigid insulated half-space. Liu et al. (2011) studied a two-dimensional thermoelastic contact problem between a rigid punch and a homogeneous half-plane with a FGM coating. In all the mentioned studies, an assumption of a half-space was adopted, which is not consistent with the real engineering practices. In fact, Choi (2009) investigated the contact problem of a functionally graded elastic layer loaded by a frictional sliding punch without considering the thermal effect, in which the importance of modeling a finite functionally graded layer was pointed out. Similar contact problems that involve a homogeneous layer bonded to or resting on a rigid foundation can be referred in a few previous works, for example, Alblas and Kuipers (1971), Conway et al. (1966), Jaffar (2002), Reina et al. (2010), and so on. In addition, it was pointed that "More interesting and practically important would be the contact problem involving frictional heating of a thermoelastic layer" (Pauk and Wozniak, 2003) and "In many cases the modeling of components of real frictional couples by a half-space is impossible. Many pairs can be often considered as a layer" (Pauk, 1999).

A corresponding thermoelastic model of a graded layer with a finite thickness on a rigid foundation contacting with a sliding rigid punch is investigated in this paper. It is assumed that the rigid flat punch slides slowly over the surface of the graded layer with all the frictional heat generated in the contact region flowing into the graded layer and the friction coefficient is a constant. Frictional force arisen in respond to the indentation force obeys the Coulomb friction law, which is totally responsible for the generated heat. The lower boundary of the graded layer is fixed to the rigid foundation. The inertia effects are neglected, which leads to the present problem belonging to the frame-work of steady-state thermoelasticity. Fourier integral transform method and the transfer matrix approach will be used to solve the present problem theoretically with the help of numerical calculations.

2. Contact model and theoretical analysis

The contact model in the present paper is shown in Fig. 1, where a graded layer with thickness h is firmly attached to a rigid foundation. The material property of the layer is graded in the thickness direction (x-axis). A flat punch of width $2a$ is pressed against the surface of the layer by a normal force P and slides to the right with a constant speed V. The frictional force Q in the contact region abides by the Coulomb-type law,

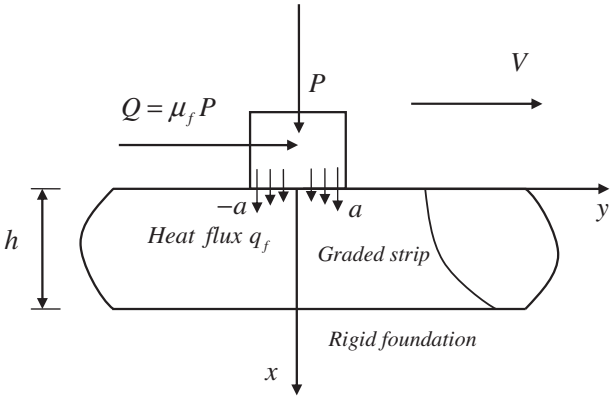

Fig. 1. Schematic of a plane strain thermoelastic contact model involving a rigid flat punch of width $2a$ sliding at a speed V on a finite graded layer of thickness h fixed on a rigid foundation. Heat transfer due to friction at the contact interface is considered with a heat flux q_f.

$$Q = \mu_f P, \tag{1}$$

where μ_f is the friction coefficient and assumed to be a constant. Thus a frictional heat flux q_f is generated in the contact area. Suppose the punch is an ideal insulator and moves slowly on the layer so that the thermal flux can be transmitted only into the graded layer in a steady state.

The graded properties of the layer are embodied by the thermal conductivity coefficient k, shear modulus μ and the thermal expansion coefficient α, which can be expressed as

$$k_2(x) = k_1 e^{\delta x}, \quad \mu_2(x) = \mu_1 e^{\beta x}, \quad \alpha_2(x) = \alpha_1 e^{\gamma x}, \tag{2}$$

where the subscript "1" denotes the surface of the layer, "2" the inside of the layer. δ, β and γ are defined to ensure the continuity of the thermoelastic parameters from the surface of the layer to the lower boundary, i.e., $x = h$. Thus we have

$$\delta = \frac{1}{h}\ln\left(\frac{k_3}{k_1}\right), \quad \beta = \frac{1}{h}\ln\left(\frac{\mu_3}{\mu_1}\right), \quad \gamma = \frac{1}{h}\ln\left(\frac{\alpha_3}{\alpha_1}\right), \tag{3}$$

where the subscript "3" denotes the lower boundary of the layer. Poisson's ratio of the graded layer is assumed to be a constant.

The model in the present paper looks like but is different from that in Choi and Paulino (2008). The relationship between the two models is independent and parallel. One of the models cannot be transferred to another, since the continuity condition of shear modulus between the graded layer and the elastic half-space has been adopted in Choi and Paulino (2008), even if the thickness of the above homogeneous layer vanishes in their model.

Denoting $u(x,y)$ and $v(x,y)$ as the displacement components in the x and y directions, respectively. $\Theta(x,y)$ is the temperature measured from the referenced stress-free temperature (temperature difference). The constitutive relations of the graded layer in terms of the displacement components $u(x,y)$, $v(x,y)$ as well as the temperature field $\Theta(x,y)$ are given as

$$\sigma_{xx} = \frac{\mu_2}{\kappa - 1}\left[(1+\kappa)\frac{\partial u}{\partial x} + (3-\kappa)\frac{\partial v}{\partial y} - 4\alpha_2^*\Theta\right], \tag{4a}$$

$$\sigma_{yy} = \frac{\mu_2}{\kappa - 1}\left[(1+\kappa)\frac{\partial v}{\partial y} + (3-\kappa)\frac{\partial u}{\partial x} - 4\alpha_2^*\Theta\right], \tag{4b}$$

$$\sigma_{xy} = \mu_2\left[\frac{\partial u}{\partial y} + \frac{\partial v}{\partial x}\right], \tag{4c}$$

where $\kappa = 3 - 4\nu, \alpha_j^* = (1+\nu)\alpha_j, (j = 1,2,3)$ for the plane strain problem and $\kappa = (3-\nu)/(1+\nu), \alpha_j^* = \alpha_j, (j = 1,2,3)$ for the plane stress case.

According to Choi and Paulino (2008), the steady-state heat conduction equation for the graded layer subjected to the frictional heating generated by the slowly sliding punch is given as

$$\nabla^2\Theta + \delta\frac{\partial\Theta}{\partial x} = 0. \tag{5}$$

The equilibrium equations are given as follows,

$$\nabla^2 u + \frac{2}{\kappa-1}\left(\frac{\partial^2 u}{\partial x^2} + \frac{\partial^2 v}{\partial x\partial y}\right) + \frac{\beta}{\kappa-1}\left[(1+\kappa)\frac{\partial u}{\partial x} + (3-\kappa)\frac{\partial v}{\partial y}\right] = \frac{4\alpha_2^* e^{\gamma x}}{\kappa-1}\left[(\beta+\gamma)\Theta + \frac{\partial\Theta}{\partial x}\right], \tag{6a}$$

$$\nabla^2 v + \frac{2}{\kappa-1}\left(\frac{\partial^2 v}{\partial y^2} + \frac{\partial^2 u}{\partial x\partial y}\right) + \beta\left(\frac{\partial v}{\partial x} + \frac{\partial u}{\partial y}\right) = \frac{4\alpha_2^* e^{\gamma x}}{\kappa-1}\frac{\partial\Theta}{\partial y}. \tag{6b}$$

For the special case of a homogeneous layer, we have $\delta = 0$, $\beta = 0$, $\gamma = 0$.

2.1. Thermal and mechanical boundary conditions

In view of the fact that the entire frictional heat flows into the graded layer through the contact area without any loss to the surroundings (Hills and Barber, 1985), the problem can be treated within the linear thermoelasticity framework. The heat flux generated by the tangential traction in the contact area is modeled to equal the rate of frictional heat generation (Joachim-Ajao and Barber, 1998), i.e.,

$$k_1\frac{\partial\Theta(0,y)}{\partial x} = -q_f(y), \quad |y| < a, \tag{7}$$

where $q_f(y)$ is related to the friction coefficient, the sliding speed and the normal stress at the interface between the punch and the graded layer,

$$q_f(y) = -\mu_f V\sigma_{xx}(0,y). \tag{8}$$

Insulation condition on the surface ($x = 0$) but outside the contact region leads to

$$k_1\frac{\partial\Theta(0,y)}{\partial x} = 0, \quad |y| > a. \tag{9}$$

On the lower interface $x = h$, we assume that the temperature remains constant for convenience, then the temperature difference at $x = h$ is

$$\Theta(h,y) = 0, \quad |y| < \infty. \tag{10}$$

For a flat punch case, the normal displacement component is known a priori within the contact area via the prescribed punch profile, i.e.,

$$u(0,y) = u_0, \quad |y| < a, \tag{11}$$

where u_0 is a constant denoting the penetration depth inside the contact region. The normal and tangential tractions beneath the punch abide by the Coulomb friction law and the external force P equals the integral of the normal traction in the contact area, i.e.,

$$\sigma_{xy}(0,y) = \mu_f\sigma_{xx}(0,y), \quad |y| \leqslant a, \tag{12}$$

$$\int_{-a}^{a}\sigma_{xx}(0,y)\mathrm{d}y = -P, \quad |y| \leqslant a, \tag{13}$$

outside the contact region, we have

$$\sigma_{xy}(0,y) = \sigma_{xx}(0,y) = 0, \quad |y| \geqslant a. \tag{14}$$

Due to the fixed condition at $x = h$, the normal and tangential displacements vanish,

$$u(h,y) = v(h,y) = 0. \tag{15}$$

2.2. Temperature field

Fourier integral transform method is adopted in the present paper in order to solve the governing equations of thermoelasticity. Transform with respect to y in Eq. (5) leads to the temperature field,

$$\Theta(x,y) = \frac{1}{2\pi}\int_{-\infty}^{+\infty}\sum_{j=1}^{2}A_j e^{\lambda_j x - \mathrm{i}sy}\mathrm{d}s, \tag{16}$$

where s is the transform variable, $\mathrm{i}^2 = -1$ and $\lambda_j(s)$ $(j = 1,2)$ are given as

$$\lambda_1(s) = -\frac{\delta}{2} + \sqrt{\frac{\delta^2}{4} + s^2}, \quad \lambda_2(s) = -\frac{\delta}{2} - \sqrt{\frac{\delta^2}{4} + s^2}, \tag{17}$$

and $A_j(s)$ $(j = 1,2)$ are unknown functions that should be determined by the thermal boundary conditions.

Considering the boundary conditions in Eqs. (7), (9), and (10) results in

$$A_1(s) = \frac{\bar{q}_f e^{\lambda_2 h}}{\lambda_1 e^{\lambda_2 h} - \lambda_2 e^{\lambda_1 h}}, \quad A_2(s) = \frac{\bar{q}_f e^{\lambda_1 h}}{\lambda_2 e^{\lambda_1 h} - \lambda_1 e^{\lambda_2 h}}, \tag{18}$$

$$\bar{q}_f(s) = -\int_{-a}^{a}\frac{q_f(\xi)}{k_1}e^{\mathrm{i}s\xi}\mathrm{d}\xi. \tag{19}$$

2.3. Mechanical field

Similarly, Fourier integral transform method can be used to solve Eqs. (6a) and (6b), which yields the displacement fields

$$u(x,y) = -\frac{\mathrm{i}}{2\pi}\int_{-\infty}^{+\infty}\sum_{j=1}^{4}B_j F_j e^{m_j x - \mathrm{i}sy}\mathrm{d}s + \frac{4\alpha_2^* e^{\gamma x}}{\kappa-1}\frac{1}{2\pi}\int_{-\infty}^{+\infty}\sum_{j=1}^{2}A_j\frac{\Phi_j}{\Delta_j}e^{\lambda_j x - \mathrm{i}sy}\mathrm{d}s, \tag{20}$$

$$v(x,y) = \frac{1}{2\pi}\int_{-\infty}^{+\infty}\sum_{j=1}^{4}B_j e^{m_j x - \mathrm{i}sy}\mathrm{d}s + \frac{4\alpha_2^* e^{\gamma x}}{\kappa-1}\frac{\mathrm{i}}{2\pi}\int_{-\infty}^{+\infty}\sum_{j=1}^{2}A_j\frac{\Omega_j}{\Delta_j}e^{\lambda_j x - \mathrm{i}sy}\mathrm{d}s, \tag{21}$$

where $B_j(s)$ $(j = 1,\ldots,4)$ are arbitrary unknown parameters. $m_j(s)$ $(j = 1,\ldots,4)$ are roots of the following characteristic equation,

$$(m^2 - s^2 + \beta m)^2 + \left(\frac{3-\kappa}{1+\kappa}\right)s^2\beta^2 = 0, \tag{22}$$

from which we have

$$m_j(s) = -\frac{\beta}{2} + \sqrt{\frac{\beta^2}{4} + s^2 - \mathrm{i}(-1)^j\beta s\left(\frac{3-\kappa}{1+\kappa}\right)^{1/2}}, \quad \mathrm{Re}(m_j) > 0, \quad j = 1,2, \tag{23a}$$

$$m_j(s) = -\frac{\beta}{2} - \sqrt{\frac{\beta^2}{4} + s^2 + \mathrm{i}(-1)^j\beta s\left(\frac{3-\kappa}{1+\kappa}\right)^{1/2}}, \quad \mathrm{Re}(m_j) < 0, \quad j = 3,4 \tag{23b}$$

and $F_j(s)$ for each $m_j(s)$ $(j = 1,\ldots,4)$ is

$$F_j(s) = \frac{(\kappa-1)(m_j^2+\beta m_j) - s^2(\kappa+1)}{s[2m_j+\beta(\kappa-1)]}. \tag{24}$$

Besides, the thermoelastic constants $\Phi_j(s)$, $\Omega_j(s)$ and $\Delta_j(s)$ $(j = 1,2)$ in the particular solutions of Eqs. (20) and (21) are expressed as

$$\Phi_j(s) = (\beta+\gamma+\lambda_j)\left[\left(\frac{\kappa-1}{\kappa+1}\right)D_j - \frac{4\kappa s^2}{\kappa^2-1}\right] + s^2 W_j,, \tag{25a}$$

$$\Omega_j(s) = s(\beta+\gamma+\lambda_j)\left[W_j + 2\beta\left(\frac{\kappa-2}{\kappa-1}\right)\right] - sD_j, \tag{25b}$$

$$\Delta_j(s) = \left[\left(\frac{\kappa-1}{\kappa+1}\right)D_j - \frac{4\kappa s^2}{\kappa^2-1}\right]D_j + s^2\left[W_j + 2\beta\left(\frac{\kappa-2}{\kappa-1}\right)\right]W_j, \tag{25c}$$

in which D_j and W_j $(j = 1,2)$ are defined as

$$D_j = \left(\frac{\kappa+1}{\kappa-1}\right)(\gamma+\lambda_j)(\beta+\gamma+\lambda_j) - s^2, \tag{26a}$$

$$W_j = \frac{2(\gamma+\lambda_j)+\beta(3-\kappa)}{\kappa-1}. \tag{26b}$$

From the above analysis, one can see that there are still four unknown parameters, i.e., $B_j(s)$ $(j = 1,\ldots,4)$. Mechanical boundary conditions of Eqs. (12)–(15) will be used to find them.

3. Solutions of the surface displacements

Similar to Choi and Paulino (2008), a transfer matrix approach is employed in this section in order to obtain the surface displacements of the graded layer subjected to arbitrary tractions and heat flux.

From the general solutions in Eqs. (20) and (21) and the constitutive relations in Eqs. (4a)–(4c), the displacement and stress components in the graded layer can be represented in a Fourier-transformed domain as

$$\mathbf{f}(x,s) = \mathbf{T}(x,s)\mathbf{a}(s) + \mathbf{f}_T(x,s), \tag{27}$$

where $\mathbf{f}(x,s)$ is a state vector containing the physical variables that need to be determined for the given constituents, $\mathbf{a}(s)$ is a vector for the unknowns in the general solutions such that

$$\mathbf{f}(x,s) = \{\bar{u}(x,s)/\mathrm{i},\ \bar{v}(x,s),\ \bar{\sigma}_{xx}(x,s)/\mathrm{i},\ \bar{\tau}_{xy}(x,s)\}^{\mathrm{T}}, \tag{28}$$

$$\mathbf{a}(s) = \{B_1(s),\quad B_2(s),\quad B_3(s),\quad B_4(s)\}^{\mathrm{T}}, \tag{29}$$

and $\mathbf{T}(x,s)$ is a 4×4 matrix, which is a function of not only the variables x and s, but also elastic parameters of the constituents, while $\mathbf{f}_T(x,s)$ is a vector representing the nonisothermal effect in Eqs. (20) and (21).

Thus, on the interface between the graded layer and the rigid foundation, the relation in Eq. (27) can be expressed as

$$\mathbf{f}(h,s) = \mathbf{T}(h,s)\mathbf{a}(s) + \mathbf{f}_T(h,s), \tag{30}$$

in which an appropriate interface condition can be given as

$$\mathbf{f}(h,s) = \{0,0,\bar{\sigma}_{xx}(h,s)/\mathrm{i},\ \bar{\tau}_{xy}(h,s)\}^{\mathrm{T}}. \tag{31}$$

For the upper surface of the graded layer, a similar relation can be written as,

$$\mathbf{f}(0,s) = \mathbf{T}(0,s)\mathbf{a}(s) + \mathbf{f}_T(0,s), \tag{32}$$

and $\mathbf{f}(0,s)$ is expressed as follows,

$$\mathbf{f}(0,s) = \{\bar{u}(0,s)/\mathrm{i},\ \bar{v}(0,s),\quad \bar{\sigma}_{xx}(0,s)/\mathrm{i},\ \bar{\tau}_{xy}(0,s)\}, \tag{33}$$

where

$$\bar{\sigma}_{xx}(0,s) = \int_{-a}^{a}\sigma_{xx}(0,y)e^{isy}\mathrm{d}y, \quad \bar{\tau}_{xy}(0,s) = \int_{-a}^{a}\tau_{xy}(0,y)e^{isy}dy. \tag{34}$$

From Eqs. (30)–(33), we can readily obtain the following relations through eliminating the unknown vector $\mathbf{a}(s)$,

$$\mathbf{f}(0,s) = \mathbf{G}(s)\mathbf{f}(h,s) + \mathbf{r}_0, \tag{35}$$

where $\mathbf{G}(s)$ is a 4×4 transfer matrix between the upper and the lower surfaces of the graded layer, $\mathbf{r}_0(s)$ is a vector of length four involving the thermal loading,

$$\mathbf{G}(s) = \mathbf{T}(0,s)\mathbf{T}^{-1}(h,s), \tag{36a}$$

$$\mathbf{r}_0 = -\mathrm{i}\mathbf{r}(s)\bar{q}_f = -\mathbf{T}(0,s)\mathbf{T}^{-1}(h,s)\mathbf{f}_T(h,s) + \mathbf{f}_T(0,s), \tag{36b}$$

The superscript "−1" denotes the inverse of a matrix and the transformed heat flux $\bar{q}_f$ has been given in Eq. (19).

By now, the unknown vector $\mathbf{a}(s)$ in equation (27) is eliminated and the transformed surface displacements $\bar{u}(0,s)$ and $\bar{v}(0,s)$ are obtained in terms of the transformed surface stresses $\bar{\sigma}_{xx}(0,s)$, $\bar{\tau}_{xy}(0,s)$ and heat flux $\bar{q}_f$. Inverse Fourier transform yields the surface displacements,

$$u(0,y) = \frac{1}{2\pi}\int_{-\infty}^{+\infty}\left[N_{11}(s)\bar{\sigma}_{xx}(0,s) + \mathrm{i}N_{12}(s)\bar{\tau}_{xy}(0,s) + L_1(s)\bar{q}_f\right]\mathrm{e}^{-isy}\mathrm{d}s, \quad |y| < +\infty, \tag{37}$$

$$v(0,y) = \frac{1}{2\pi}\int_{-\infty}^{+\infty}\left[-\mathrm{i}N_{21}(s)\bar{\sigma}_{xx}(0,s) + N_{22}(s)\bar{\tau}_{xy}(0,s) - \mathrm{i}L_2(s)\bar{q}_f\right]\mathrm{e}^{-isy}\mathrm{d}s, \quad |y| < +\infty, \tag{38}$$

where $N_{jk}(s)$ $(j,k = 1,2)$ are the elements of a 2×2 matrix $\mathbf{N}(s)$. $L_j(s)$ $(j = 1,2)$ are those of a vector of two units in length $\mathbf{L}(s)$,

$$\mathbf{N}(s) = \begin{bmatrix} G_{13} & G_{14} \\ G_{23} & G_{24}\end{bmatrix}\begin{bmatrix} G_{33} & G_{34} \\ G_{43} & G_{44}\end{bmatrix}^{-1}, \tag{39}$$

$$\mathbf{L}(s) = \begin{Bmatrix} r_1 \\ r_2\end{Bmatrix} - \begin{bmatrix} G_{13} & G_{14} \\ G_{23} & G_{24}\end{bmatrix}\begin{bmatrix} G_{33} & G_{34} \\ G_{43} & G_{44}\end{bmatrix}^{-1}\begin{Bmatrix} r_3 \\ r_4\end{Bmatrix}, \tag{40}$$

It is found that the matrix $\mathbf{N}(s)$ and vector $\mathbf{L}(s)$ depend only on the elastic parameters of the constituents and thermoelastic parameters of the graded layer, respectively.

4. Solutions of the contact stresses and stress intensity factors

Considering the relations in Eqs. (19) and (34) and differentiating with respect to the variable y, the surface displacements in Eqs. (37) and (38) can be written as,

$$\frac{\partial u(0,y)}{\partial y} = -\frac{1}{2\pi}\int_{-a}^{+a}\left[\mathrm{i}I_{11}(y,r)\sigma_{xx}(0,r) - I_{12}(y,r)\tau_{xy}(0,r) + \mathrm{i}I_{13}(y,r)q_f(r)\right]\mathrm{d}r, \tag{41}$$

$$\frac{\partial v(0,y)}{\partial y} = -\frac{1}{2\pi}\int_{-a}^{+a}\left[I_{21}(y,r)\sigma_{xx}(0,r) + \mathrm{i}I_{22}(y,r)\tau_{xy}(0,r) + I_{23}(y,r)q_f(r)\right]\mathrm{d}r, \tag{42}$$

where the kernels in the above equations are,

$$I_{jk}(y,r) = \int_{-\infty}^{+\infty} sN_{jk}(s)\mathrm{e}^{\mathrm{i}s(r-y)}\mathrm{d}s, \quad j = 1,2 \quad k = 1,2 \tag{43}$$

$$I_{j3}(y,r) = -\frac{1}{k_1}\int_{-\infty}^{+\infty} sL_j(s)\mathrm{e}^{\mathrm{i}s(r-y)}\mathrm{d}s, \quad j = 1,2 \tag{44}$$

When s approaches to infinity or zero, $N_{jk}(s)$ $(j=1,2,\ k=1,2)$ and $L_j(s)$ $(j=1,2)$ have the following asymptotic behaviors,

$$\lim_{|s|\to\infty} sN_{11} = \Lambda_{11}\frac{|s|}{s}, \quad \lim_{|s|\to\infty} sN_{22} = \Lambda_{22}\frac{|s|}{s}. \tag{45a}$$

$$\lim_{|s|\to\infty} sN_{12} = \Lambda_{12}, \quad \lim_{|s|\to\infty} sN_{21} = \Lambda_{21} \tag{45b}$$

$$\lim_{|s|\to\infty} sL_1 = \lim_{|s|\to\infty} sL_2 = 0, \tag{45c}$$

$$\lim_{|s|\to 0} sL_1 = L_1^0, \quad \lim_{|s|\to 0} sL_2 = L_2^0 \tag{45d}$$

where $\Lambda_{11}=\Lambda_{22}=-\frac{(\kappa+1)}{4\mu_1}$, $\Lambda_{12}=\Lambda_{21}=-\frac{(\kappa-1)}{4\mu_1}$, $L_1^0=-\frac{2\alpha_3^*}{k_3}\frac{1}{s}$ and $L_2^0=-\frac{2\alpha_3^*}{k_3}\frac{\kappa}{\kappa+1}\frac{1}{|s|}$.

Denote $\delta(\cdot)$ as the Dirac delta function. Separating the leading terms from the kernels in Eq. (45) and using the following Fourier generalized functions

$$\int_0^\infty \sin[s(r-y)]\mathrm{d}s = \frac{1}{r-y}, \quad \int_0^\infty \cos[s(r-y)]\mathrm{d}s = \pi\delta(r-y), \tag{46}$$

Eqs. (41) and (42) can be written as,

$$\begin{aligned}\frac{\partial u(0,y)}{\partial y} &= \Lambda_{12}\tau_{xy}(0,y) + \frac{1}{\pi}\int_{-a}^{a}\frac{\Lambda_{11}}{r-y}\sigma_{xx}(0,r)\mathrm{d}r \\ &+ \frac{1}{\pi}\int_{-a}^{a}\left[K_{11}(r,y)\sigma_{xx}(0,r) + K_{12}(r,y)\tau_{xy}(0,r) - \frac{1}{k_1}K_{13}(r,y)q_f(r)\right]\mathrm{d}r.\end{aligned} \tag{47a}$$

$$\begin{aligned}\frac{\partial v(0,y)}{\partial y} &= -\Lambda_{21}\sigma_{xx}(0,y) + \frac{1}{\pi}\int_{-a}^{a}\frac{\Lambda_{22}}{r-y}\tau_{xy}(0,r)\mathrm{d}r \\ &- \frac{1}{\pi}\int_{-a}^{a}\left[K_{21}(r,y)\sigma_{xx}(0,r) - K_{22}(r,y)\tau_{xy}(0,r) - \frac{1}{k_1}K_{23}(r,y)q_f(r)\right]\mathrm{d}r,\end{aligned} \tag{47b}$$

where $K_{mn}(r,y)$ $(m,n=1,2)$ are defined as

$$K_{mn}(r,y) = \begin{cases}\int_0^\infty [sN_{mn}(s)-\Lambda_{mn}]\sin[s(r-y)]\mathrm{d}s, & m=n \\ \int_0^\infty [sN_{mn}(s)-\Lambda_{mn}]\cos[s(r-y)]\mathrm{d}s, & m\neq n\end{cases} \tag{48a}$$

$$K_{13}(r,y) = \int_0^\infty sL_1(s)\sin[s(r-y)]\mathrm{d}s, \tag{48b}$$

$$K_{23}(r,y) = \int_0^\infty sL_2(s)\cos[s(r-y)]\mathrm{d}s. \tag{48c}$$

Take into consideration the relations in Eqs. (8) and (12), the following equations should be satisfied inside the contact area

$$\sigma_{xx}(0,y) = -p(y), \quad |y|<a, \tag{49}$$

$$\sigma_{xy}(0,y) = -\mu_f p(y), \quad |y|<a, \tag{50}$$

$$q_f(y) = \mu_f V p(y), \quad |y|<a, \tag{51}$$

where $p(y)$ denotes the normal traction in the contact region.

Then, Eq. (47a) can be rewritten as,

$$\mu_f\Lambda_{12}p(y) + \frac{1}{\pi}\int_{-a}^{a}\frac{\Lambda_{11}}{r-y}p(r)\mathrm{d}r + \frac{1}{\pi}\int_{-a}^{a}Q_1(r,y)p(r)\mathrm{d}r = -\frac{\partial u(0,y)}{\partial y}, \tag{52}$$

where the bounded kernel $Q_1(r,y)$ is given by

$$Q_1(r,y) = K_{11}(r,y) + \mu_f K_{12}(r,y) + \frac{\mu_f V}{k_1}K_{13}(r,y). \tag{53}$$

In addition, the mechanical boundary condition in Eq. (13) should be satisfied. We solve Eqs. (52) and (13) by introducing the following non-dimensional quantities,

$$\begin{cases} r=a\eta, \quad y=a\xi, \quad -a<(r,y)<a, \quad -1<(\eta,\xi)<1 \\ Q^*(\eta,\xi) = aQ_1(\eta,\xi)\end{cases} \tag{54}$$

Then, Eqs. (52) and (13) become

$$\begin{aligned}&\mu_f\Lambda_{12}p(\xi) + \frac{1}{\pi}\int_{-1}^{1}\frac{\Lambda_{11}}{\eta-\xi}p(\eta)\mathrm{d}\eta + \frac{1}{\pi}\int_{-1}^{1}Q^*(\eta,\xi)p(\eta)\mathrm{d}\eta \\ &= -\frac{1}{a}\frac{\partial u(0,\xi)}{\partial\xi}, \quad |\xi|<1,\end{aligned} \tag{55}$$

$$\int_{-1}^{1}p(\xi)\mathrm{d}\xi = \frac{P}{a}. \tag{56}$$

Due to the Cauchy-type singular kernel in the integral equation, the solution to Eqs. (55) and (56) can be expressed in terms of Jacobi Polynomials, i.e.,

$$p(\xi) = w(\xi)\sum_{j=0}^{\infty}c_j P_j^{(\beta_1,\beta_2)}(\xi), \quad |\xi|<1. \tag{57}$$

in which the weight function $w(\xi)=(1-\xi)^{\beta_1}(1+\xi)^{\beta_2}$ and parameters c_j are unknown. $P_j^{(\beta_1,\beta_2)}(\cdot)$ are Jacobi Polynomials corresponding to the weight function $w(\xi)$. The superscripts β_1 and β_2 are determined from the physics of the problem, i.e.,

$$\begin{cases}\theta>0: & \beta_1=-\frac{\varepsilon}{\pi} \quad \beta_2=\frac{\varepsilon}{\pi}-1 \\ \theta=0: & \beta_1=-\frac{1}{2} \quad \beta_2=-\frac{1}{2} \\ \theta<0: & \beta_1=\frac{\varepsilon}{\pi}-1 \quad \beta_2=-\frac{\varepsilon}{\pi}\end{cases}, \tag{58}$$

where $\theta=\frac{\mu_f\Lambda_{12}}{\Lambda_{11}}$ and $\tan\varepsilon=|\frac{1}{\theta}|$. It is easy to find that β_1 and β_2 as indexes of the stress singularity at the leading $(y=a)$ and trailing $(y=-a)$ contact edges, respectively, depend only on the friction coefficient and Poisson's ratio, the same as those in the isothermal counterpart case (Choi, 2009).

Considering Eq. (11) and the following property of Jacobi Polynomials,

$$\begin{aligned}&\mu_f\Lambda_{12}w(\xi)P_j^{(\beta_1,\beta_2)}(\xi) + \frac{1}{\pi}\int_{-1}^{1}\frac{\Lambda_{11}}{\eta-\xi}w(\xi)P_j^{(\beta_1,\beta_2)}(\xi)\mathrm{d}\eta \\ &= -\frac{2^{-1}\Lambda_{11}}{\sin(\pi\beta_1)}P_{j-1}^{(-\beta_1,-\beta_2)}(\xi), \quad |\xi|<1,\end{aligned} \tag{59}$$

substituting Eq. (57) into Eq. (55) yields

$$\sum_{j=0}^{\infty}\left[\frac{-\Lambda_{11}}{2\sin(\pi\beta_1)}P_{j-1}^{(-\beta_1,-\beta_2)}(\xi) + Q_j^*(\xi)\right] \quad c_j = 0, \tag{60}$$

where

$$Q_j^*(\xi) = \frac{1}{\pi}\int_{-1}^{1}Q^*(\eta,\xi)w(\eta)P_j^{(\beta_1,\beta_2)}(\eta)\mathrm{d}\eta. \tag{61}$$

Substituting Eq. (57) into (56) and employing the following orthogonality property of Jacobi Polynomials

$$\int_{-1}^{1}w(\xi)P_j^{(\beta_1,\beta_2)}(\xi)P_k^{(\beta_1,\beta_2)}(\xi)\mathrm{d}\xi = \theta_j^{(\beta_1,\beta_2)}\delta_{jk}, \quad j,k=0,1,2,\ldots, \tag{62}$$

we have

$$c_0\theta_0^{(\beta_1,\beta_2)} = \frac{P}{a}, \tag{63}$$

where

$$\theta_j^{(\beta_1,\beta_2)} = \begin{cases} \int_{-1}^{1} w(\xi)\mathrm{d}\xi = \frac{2^{\beta_1+\beta_2+1}\Gamma(\beta_1+1)\Gamma(\beta_2+1)}{\Gamma(\beta_1+\beta_2+2)}, & j=0, \\ \frac{2^{\beta_1+\beta_2+1}\Gamma(j+\beta_1+1)\Gamma(j+\beta_2+1)}{(2j+\beta_1+\beta_2+1)j!\Gamma(j+\beta_1+\beta_2+1)}, & j \geqslant 1, \end{cases} \tag{64}$$

and δ_{jk} is the Kronecker delta function.

Truncating the series in Eq. (60) at $j = N$ and selecting collocation points (Guler and Erdogan, 2004, 2006, 2007) $\xi_m (m = 1,2,\ldots,N)$ as roots of the following Jacobi Polynomials

$$P_N^{(-\beta_1,-\beta_2)}(\xi_m) = 0, \tag{65}$$

and using the following defined variables,

$$c_j^* = \frac{c_j}{2\sigma_0}, \quad \sigma_0 = \frac{P}{2a}, \tag{66}$$

Eqs. (60) and (63) can be written as

$$\sum_{j=0}^{N}\left[\frac{-\Lambda_{11}}{2\sin(\pi\beta_1)}P_{j-1}^{(-\beta_1,-\beta_2)}(\xi_m) + Q_j^*(\xi_m)\right]c_j^* = 0, \quad c_0^*\theta_0^{(\beta_1,\beta_2)} = 1, \tag{67}$$

which consists of $N+1$ linear algebraic equations for $N+1$ unknown constants c_j^* $(j = 0,1,\ldots,N)$.

Based on the solution of Eq. (67), $p(y)$ in Eq. (57) can be approximately given as

$$p(y) = 2\sigma_0\left(1-\frac{y}{a}\right)^{\beta_1}\left(1+\frac{y}{a}\right)^{\beta_2}\sum_{j=0}^{N}c_j^*P_j^{(\beta_1,\beta_2)}\left(\frac{y}{a}\right). \tag{68}$$

Then, the expression for the in-plane stress component $\sigma_{yy}(0,y)$ under the punch can be obtained from the constitutive relations in Eq. (4b) and Eqs. (47a) and (47b) as

$$\sigma_{yy}(0,y) = -p(y) + \frac{2\mu_f}{\pi}\int_{-a}^{a}\frac{1}{r-y}p(r)\mathrm{d}r - \frac{2}{\pi}\int_{-a}^{a}\frac{1}{\Lambda_{22}}Q_2(r,y)p(r)\mathrm{d}r + \frac{2\alpha_1^*}{\Lambda_{22}}\Theta(0,y), \quad |y| < \infty, \tag{69}$$

where $Q_2(r,y)$ is

$$Q_2(r,y) = K_{21}(r,y) - \mu_f K_{22}(r,y) + \frac{\mu_f V}{k_1}K_{23}(r,y). \tag{70}$$

The stress intensity factors near the contact edges may be defined as

$$F_I(a) = \lim_{y\to a}\frac{p(y)}{2^{\beta_2}}(a-y)^{-\beta_1} = \frac{2\sigma_0}{a^{\beta_1}}\sum_{j=0}^{\infty}c_j^*P_j^{(\beta_1,\beta_2)}(1), \tag{71}$$

$$F_I(-a) = \lim_{y\to -a}\frac{p(y)}{2^{\beta_1}}(a+y)^{-\beta_2} = \frac{2\sigma_0}{a^{\beta_2}}\sum_{j=0}^{\infty}c_j^*P_j^{(\beta_1,\beta_2)}(-1). \tag{72}$$

5. Several kinds of special cases

(i) Three kinds of special cases, (i) an isothermal case with a graded layer (Choi, 2009), (ii) a homogeneous layer case, (iii) a graded layer with an infinite thickness, can be deduced from the present general model.

(ii) From the thermal boundary condition in Eq. (8), one can find that either $V = 0$ or friction coefficient $\mu_f = 0$ will lead to zero heat flux. Then the effect of the temperature field vanishes and all the terms related to temperature should be deleted. When the friction coefficient vanishes, i.e., $\mu_f = 0$, the second kind Cauchy-type singular integral equation (55) will reduce to the first kind one for the isothermal frictionless contact case. The stress singularity at the contact edges becomes the classical one, i.e., $\beta_1 \to -1/2$, $\beta_2 \to -1/2$. When $V = 0$, the present problem will degenerate to the one in Choi (2009). Numerical comparisons are given in the following section.

(iii) When the graded parameters δ, β and γ vanish, the graded layer will become a homogeneous one. Solutions to the corresponding model of a homogeneous layer on a rigid foundation can be found in the following numerical analysis as a special case for comparison, in which we take $k_3/k_1 = 1$, $\mu_3/\mu_1 = 1$ and $\alpha_3/\alpha_1 = 1$.

For the case with an infinite graded layer, i.e., $h \to \infty$. A positive or negative real part in the characteristic roots related to the heat conduction equation in Eq. (17) and those related to the thermoelastic governing equations in Eqs. (23a) and (23b) can be distinguished. In the case of $h \to \infty$, the terms corresponding to roots with a positive real part in right sides of the temperature and mechanical displacement equations (16), (20), (21) will vanish and only the terms related to roots with a negative real part remain. Thus, only two of $B_j(s)$ $(j = 1, \ldots, 4)$ and one of $A_j(s)$ $(j = 1,2)$ are nonzero. The nonzero $A_j(s)$ and $B_j(s)$ can be determined by the boundary conditions on the contact interface $(x = 0)$.

Using a similar analysis in Section 3 will result in a pair of Cauchy-type singular integral equations of the second kind as Eq. (47). Numerical solutions can also be found for the infinite graded layer case, which can be approximately represented by the case of $a \ll h$. Although the model in the present paper is different from that in Choi and Paulino (2008), both the present model and that in Choi and Paulino (2008) can be degenerated to the same special case, i.e., the contact problem between a rigid punch and a graded half-space.

Furthermore, closed-form solutions for the case of a rigid flat punch on a homogeneous half-space without thermo effects can be found from the present general model (Guler and Erdogan, 2004),

$$\frac{\sigma_{xx}(0,y)}{\sigma_0} = \frac{2\sin\pi\beta_1}{\pi}\left(1-\frac{y}{a}\right)^{\beta_1}\left(1+\frac{y}{a}\right)^{\beta_2}, \tag{73}$$

$$\frac{\sigma_{yy}(0,y)}{\sigma_0} = \frac{2\sin\pi\beta_1}{\pi}\begin{cases}\left(1-\frac{y}{a}\right)^{\beta_1}\left(1+\frac{y}{a}\right)^{\beta_2}+\frac{2\mu_f}{\pi}L_f(y), & -a<y<a, \\ \frac{2\mu_f}{\pi}L_f(y), & |y|>a,\end{cases} \tag{74}$$

where we have

$$L_f(y) = \begin{cases} -\left(1-\frac{y}{a}\right)^{\beta_1}\left(-1-\frac{y}{a}\right)^{\beta_2}, & -\infty<y<-a, \\ \left(1-\frac{y}{a}\right)^{\beta_1}\left(1+\frac{y}{a}\right)^{\beta_2}\cos\pi\beta_1, & -a<y<a, \\ \left(\frac{y}{a}-1\right)^{\beta_1}\left(1+\frac{y}{a}\right)^{\beta_2}, & a<y<\infty \end{cases} \tag{75}$$

and the corresponding stress intensity factors near the contact edges in this case can be found as

$$F_1(a) = -\frac{2\sigma_0}{\pi a^{\beta_1}}\sin\pi\beta_1, \tag{76}$$

$$F_1(-a) = -\frac{2\sigma_0}{\pi a^{\beta_2}}\sin\pi\beta_1. \tag{77}$$

6. Numerical analysis

Numerical calculations are carried out in order to analyze the singularities near the contact edges, the stress intensity factors, the distributions of stresses and temperatures under the rigid punch. According to Giannakopoulos and Suresh (1997a, 1997b), the value of Poisson's ratio has no obvious influence on the contact behavior. $\nu = 0.3$ is assumed in the following analysis.

Comparing to the above mentioned isothermal model proposed by Choi (2009), the thermoelastic contact one evolves more thermal parameters. We take $k_1/k_3 = 0.1125$, $\alpha_1/\alpha_3 = 0.6903$ in the present paper. According to Choi (2009), we adopt the shear

modulus ratio $\mu_1/\mu_3 = 0.2$ for comparison analysis, unless otherwise stated.

For thermoelastic contact problems, the excessive amount of heat flux between the contacting bodies may give rise to the separation of contacting surfaces, enforcing the contact stress distribution to turn into positive and tensile near the contact edges (Barber and Comninou, 1989). Thus, slow sliding speed of the punch and small friction coefficient are chosen in order to avoid such a phenomenon (Joachim-Ajao and Barber, 1998).

6.1. Validation study

In order to valid our following results, the contact problem between a rigid punch and a functionally graded elastic layer based on a rigid substrate is taken for comparison first (Choi, 2009), in which the thermal effect was not considered. We only need to assume $V = 0$ in our model. The same material parameters as those in Choi (2009) are adopted. It is found that the reduced result of the present model is well consistent with the Choi's one (2009).

Another special case of a rigid flat punch on a homogeneous half-space without considering the thermo effect is further considered (Guler and Erdogan, 2004). We only need to take the thickness as infinity in our model. Excellent agreement is also found between the present model and the Guler and Erdogan's one (2004).

As for the thermocontact analysis of a homogeneous medium, Pauk and Wozniak (2003) have investigated the contact problem between a layer and a rigid punch with frictional heat effects, where the heat flux at the lower interface is given. While in the present model, the temperature at the lower interface is given. Thus, direct degeneration from our model to the Pauk and Wozniak's one is not easy and comparison between the present model and the case of a homogeneous medium cannot be presented directly.

6.2. Effects of ratio of shear modulus, sliding speed, friction coefficient and geometric parameter on distributions of contact stress

From the boundary conditions (7)-(15) and governing equations (4)-(6), one can see that the solutions of the present problem depends on the ratio of shear moduli (μ_1/μ_3), dimensionless sliding speed ($v_0 = \mu_1\alpha_1^* Va/k_1(\kappa+1)$), the half width of the sliding punch (a/h) and friction coefficient (μ_f), the effects of which on the stress singularities, the stress intensity factors at the contact edges and the stress distributions under the sliding punch are analyzed numerically.

Table 1
Stress singularities β_1, β_2 and the non-dimensional stress intensity factors $F_I(a)/F_{01}$, $F_I(-a)/F_{02}$ at the contact edges for different values of μ_1/μ_3 and fixed $v_0 = 0.2$, $a/h = 0.2$ and $\mu_f = 0.5$.

	$\mu_1/\mu_3 = 0.2$ $\beta_1 = -0.4548$ $\beta_2 = -0.5452$	$\mu_1/\mu_3 = 1$ $\beta_1 = -0.4548$ $\beta_2 = -0.5452$	$\mu_1/\mu_3 = 3$ $\beta_1 = -0.4548$ $\beta_2 = -0.5452$	$\mu_1/\mu_3 = 5$ $\beta_1 = -0.4548$ $\beta_2 = -0.5452$
$F_I(a)/F_{01}$	0.2081	0.2583	0.3052	0.3315
$F_I(-a)/F_{02}$	0.2024	0.2608	0.3154	0.3462

Fig. 2(a) and (b) give the distributions of the non-dimensional contact pressure $\sigma_{xx}(0,y)/\sigma_0$ and in-plane surface stress component $\sigma_{yy}(0,y)/\sigma_0$, respectively, where σ_0 is the average contact pressure, for different ratios of shear moduli μ_1/μ_3. It is easy to find that serious stress concentration does exist near the contact edges. Stress singularities at the trailing ($x = -a$) and leading ($x = a$) contact edges can be determined from Eq. (58) to be $\beta_2 = -0.5452$ and $\beta_1 = -0.4548$, respectively. More significant stress concentration at the trailing edge than the leading one is reflected in Fig 2(a). Furthermore, larger ratio of shear modulus, μ_1/μ_3, results in more serious stress concentration at both contact edges, while the contact pressure is reduced at the center of contact area with an increasing μ_1/μ_3. Table 1 presents the non-dimensional stress intensity factors $F_I(a)/F_{01}$ and $F_I(-a)/F_{02}$ varying with the ratio of modulus μ_1/μ_3, where $F_{01} = Pa^{\beta_2}$ and $F_{02} = Pa^{\beta_1}$. From Table 1, we find that the non-dimensional stress intensity factors at both edges increase with an increasing μ_1/μ_3. That is to say the non-dimensional stress intensity factors increases if the stiffness of the graded layer surface increases for a fixed stiffness of the lower surface of the graded layer. It is well known that, in sliding contact problem, the in-plane surface stress behind the trailing edge ($y < -a$) is more likely to be tensile, whereas it is compressive in front of the leading edge ($y > a$). Fig. 2(b) clearly shows that the in-plane surface stress is unbounded and discontinuous at both contact edges, and both the in-plane tensile surface stress behind the trailing edge and the compressive one in front of the leading edge improve with a larger value of μ_1/μ_3 comparing to the homogeneous case, i.e., $\mu_1/\mu_3 = 1$. From the fretting mechanics point of view, surface cracking caused by friction will inevitably lead to fretting fatigue. It is easy to conclude that a graded layer with gradually increasing stiffness in the thickness direction, i.e., $\mu_1/\mu_3 < 1$, will have less possibility for crack initiation and propagation, which qualitatively agrees with the experiment results given by Suresh et al. (1999). Thus, it is reasonable to design a graded layer

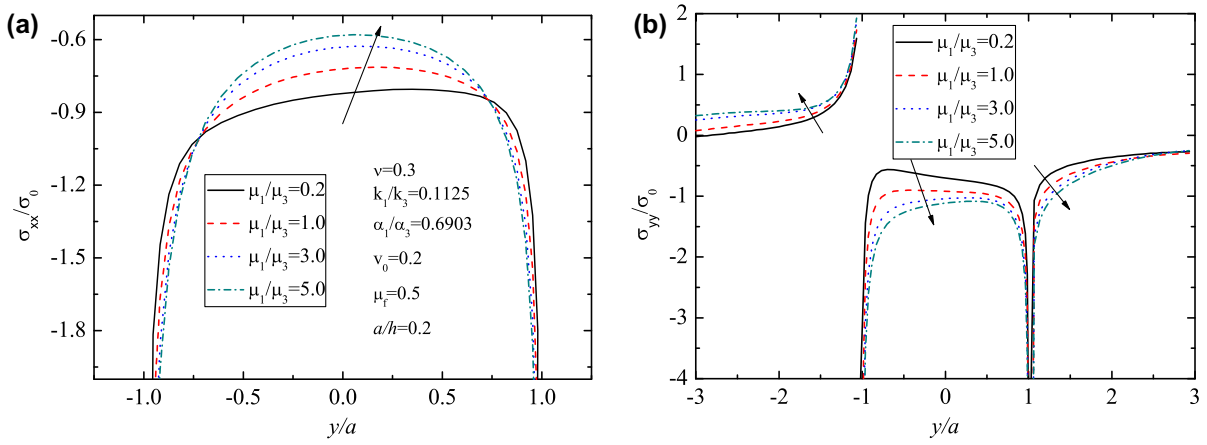

Fig. 2. Distributions of the non-dimensional contact stresses along the contact interface for different shear modulus ratios μ_1/μ_3 with fixed values $v_0 = 0.2$, $a/h = 0.2$, $\mu_f = 0.5$. (a) For the contact pressure $\sigma_{xx}(0,y)/\sigma_0$; (b) For the in-plane stress $\sigma_{yy}(0,y)/\sigma_0$, where $\sigma_0 = P/2a$.

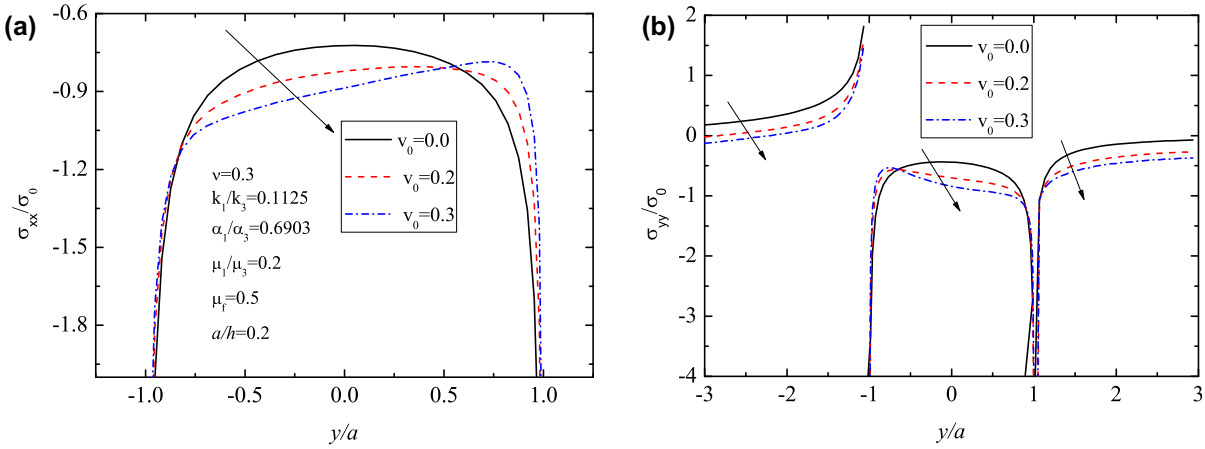

Fig. 3. Distributions of the non-dimensional contact stresses along the contact interface for different non-dimensional sliding speeds v_0 with fixed values $\mu_1/\mu_3 = 0.2$, $a/h = 0.2$, $\mu_f = 0.5$. (a) For the contact pressure $\sigma_{xx}(0,y)/\sigma_0$; (b) For the in-plane stress $\sigma_{yy}(0,y)/\sigma_0$, where $\sigma_0 = P/2a$.

Table 2
Stress singularities β_1, β_2 and the non-dimensional stress intensity factors $F_I(a)/F_{01}$, $F_I(-a)/F_{02}$ at the contact edges for different values of v_0 with fixed $\mu_1/\mu_3 = 0.2(\mu_1/\mu_3 = 3)$, $a/h = 0.2$ and $\mu_f = 0.5$.

	$\mu_1/\mu_3 = 0.2$, $\beta_1 = -0.4548$, $\beta_2 = -0.5452$		$\mu_1/\mu_3 = 3$, $\beta_1 = -0.4548$, $\beta_2 = -0.5452$	
	$F_I(a)/F_{01}$	$F_I(-a)/F_{02}$	$F_I(a)/F_{01}$	$F_I(-a)/F_{02}$
$v_0 = 0.0$	0.2857	0.2402	0.3634	0.3408
$v_0 = 0.2$	0.2081	0.2024	0.3052	0.3154
$v_0 = 0.3$	0.1601	0.1839	0.2726	0.3025

with a softer surface in order to prevent cracking damage induced by sliding friction. Comparing to the isothermal case investigated by Choi (2009), it is found that the variation tendency of the contact stress varying with the shear modulus ratio in both models is much similar. However, it is found that the effects of μ_1/μ_3 on the variation tendency of the stress intensity factor and the in-plane surface stress are totally opposite to Choi and Paulino (2008).

Effects of the dimensionless sliding speed v_0 on the distributions of contact pressure and in-plane surface stress are shown in Fig. 3, which corresponds to the case with $\mu_1/\mu_3 < 1$, i.e., the shear modulus increasing from the layer surface to the lower boundary of the layer. When the thermal effect is taken into consideration induced by an increasing sliding speed of the punch, the distribution of the contact pressure tends to significantly skew near the leading contact edge. The corresponding stress intensity factors at both contact edges, $F_I(a)/F_{01}$ and $F_I(-a)/F_{02}$ are given in the left column of Table 2, both of which decrease with an increasing v_0. A rapider reduction can be observed for $F_I(a)/F_{01}$ than $F_I(-a)/F_{02}$. Furthermore, the in-plane stress behind the trailing edge ($y < -a$) exhibits a tensile and unbounded behavior either for a large or small sliding speed, even for a stationary one. When the punch is stationary, i.e., $v_0 = 0.0$, the present result is consistent with Choi (2009).

Comparing to Fig. 3 and the left column of Table 2, Fig. 4 and the right column of Table 2 give the distributions of contact stress and stress intensity factors for the case with $\mu_1/\mu_3 > 1$. Similar phenomena can be found in both cases. It is interesting to find that the stress intensity factor at the leading edge is larger than that at the trailing edge when v_0 is under some value in both cases of $\mu_1/\mu_3 < 1$ and $\mu_1/\mu_3 > 1$. However, the phenomenon changes essentially with an increasing sliding speed. The present result is different from that of a homogeneous coating on a homogeneous half space with a graded interlayer in Choi and Paulino (2008). The main reason is that, in Choi and Paulino (2008), the numerical model can be looked macroscopically as a graded half-space varying from a hard surface to a soft bottom, while in the present model, no matter $\mu_1/\mu_3 < 1$ or $\mu_1/\mu_3 > 1$, the total model can always be

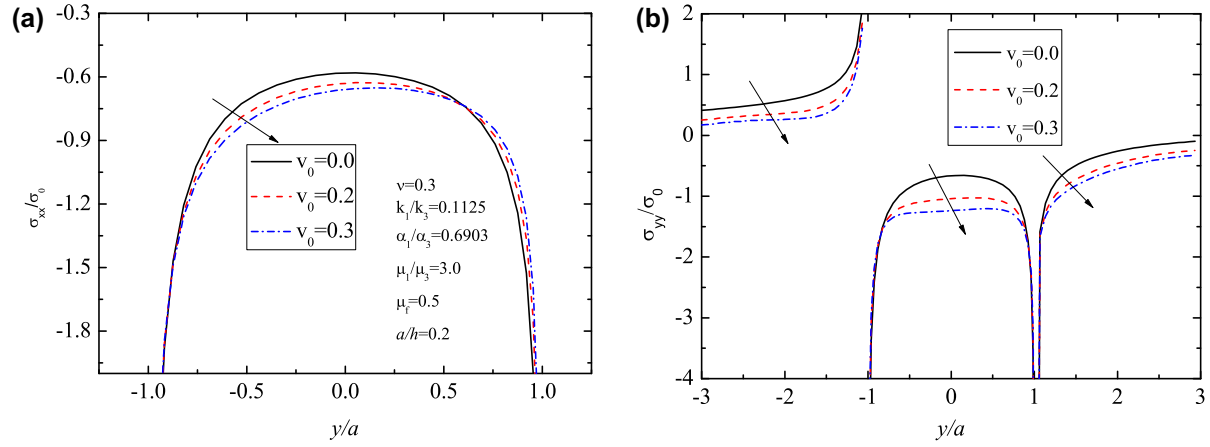

Fig. 4. Distributions of the non-dimensional contact stresses along the contact interface for different non-dimensional sliding speeds v_0 with fixed values $\mu_1/\mu_3 = 3$, $a/h = 0.2$, $\mu_f = 0.5$. (a) For the contact pressure $\sigma_{xx}(0,y)/\sigma_0$; (b) For the in-plane stress $\sigma_{yy}(0,y)/\sigma_0$, where $\sigma_0 = P/2a$.

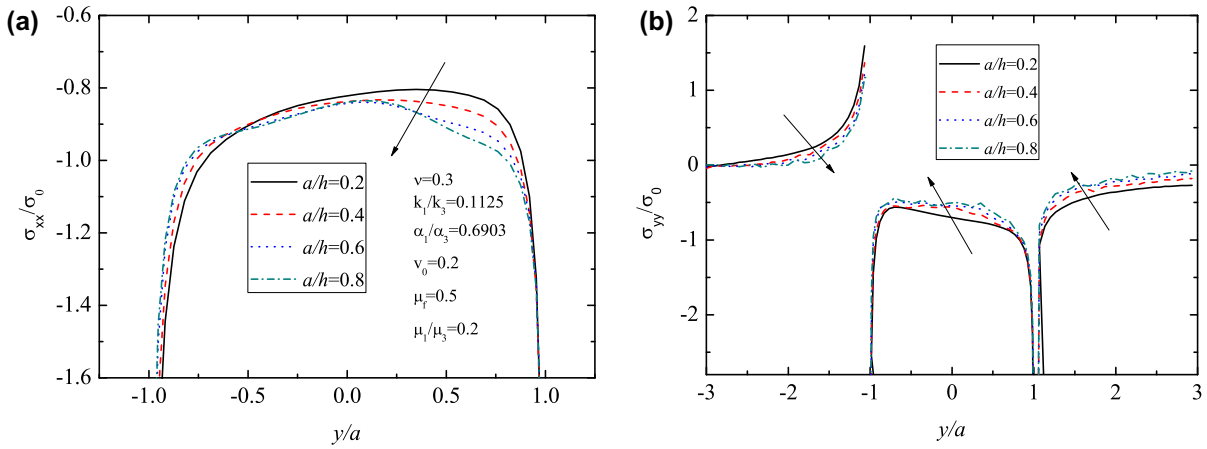

Fig. 5. Distributions of the non-dimensional contact stresses along the contact interface for different non-dimensional contact half-widths a/h with fixed values $\mu_1/\mu_3 = 0.2$, $v_0 = 0.2$, $\mu_f = 0.5$. (a) For the contact pressure $\sigma_{xx}(0,y)/\sigma_0$; (b) For the in-plane stress $\sigma_{yy}(0,y)/\sigma_0$, where $\sigma_0 = P/2a$.

Table 3
The non-dimensional stress intensity factors $F_I(a)/F_{01}$, $F_I(-a)/F_{02}$ at the contact edges for different values of a/h with fixed $\mu_1/\mu_3 = 0.2$, $v_0 = 0.2$ and $\mu_f = 0.5$.

	$a/h = 0.2$	$a/h = 0.4$	$a/h = 0.6$	$a/h = 0.8$
$F_I(a)/F_{01}$	0.2081	0.2051	0.1982	0.1938
$F_I(-a)/F_{02}$	0.2024	0.1752	0.1538	0.1430

regarded as a macroscopically graded half-space varying from a soft surface to a rigid bottom due to the rigid substrate. From this point of view, either the present results or those in Choi and Paulino (2008) agree qualitatively with Guler and Erdogan (2004), in which both phenomena were discussed but for a different problem. In addition, the in-plane tensile stress, as shown in Fig. 3(b) and Fig. 4(b), decreases with an increasing sliding speed, which indicates a suppression tendency of the aforementioned surface cracking.

The distributions of the contact pressure and the in-plane stress influencing by the non-dimensional contact width a/h are shown in Fig. 5(a) and (b), respectively. From Fig. 5(a), one can see that the surface contact stress concentration is weakened at both the contact edges when the value of a/h increases. This tendency is represented clearly by the non-dimensional stress intensity factors $F_I(a)/F_{01}$ and $F_I(-a)/F_{02}$ given in Table 3. Fig. 5(b) indicates that decreasing the thickness of the graded layer can suppress surface cracking at the trailing edge due to decreasing tensile stress.

When the friction coefficient μ_f changes from 0.1 to 0.8 and $\mu_1/\mu_3 = 0.2$ and $a/h = 0.2$ are determined, variations of contact stress under the punch and the stress intensity factors near both contact edges are given in Fig. 6 and Table 4, respectively. One can see that the stress singularity at the trailing end (β_2) becomes stronger and that at the leading end (β_1) becomes weaker than that for the corresponding frictionless case. The in-plane surface stress tends to change the sign, i.e., from compressive to tensile, behind the trailing edge ($y < -a$), while the compressive stress before the leading edge ($y > a$) becomes stronger when the friction coefficient increases as shown in Fig 6(b). It means that surface cracking is easy to happen for the case with a large friction coefficient.

6.3. Effects of thermal parameters on contact stresses

Figs. 7 and 8 are given in order to take into account the influences of thermal parameters on the mechanical fields. The non-dimensional thermal expansion coefficient α_1/α_3 and thermal conductivity coefficient k_1/k_3 are chosen as variables, respectively. The corresponding non-dimensional stress intensity factors can be found in Table 5 for different α_1/α_3 with a fixed $k_1/k_3 = 0.1125$ and different k_1/k_3 with a determined $\alpha_1/\alpha_3 = 0.6903$, respectively.

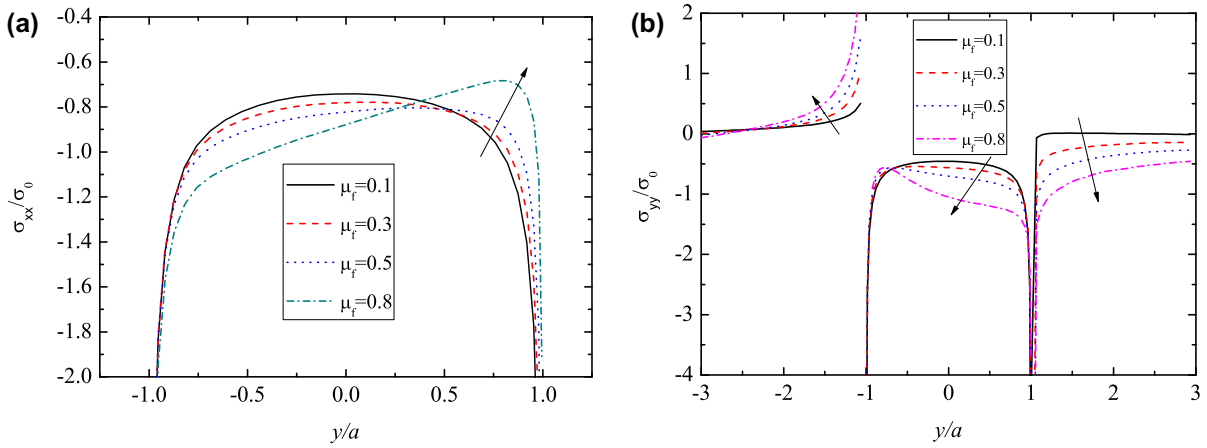

Fig. 6. Distributions of the non-dimensional contact stresses along the contact interface for different friction coefficients μ_f with fixed values $\mu_1/\mu_3 = 0.2$, $v_0 = 0.2$, $a/h = 0.2$. (a) For the contact pressure $\sigma_{xx}(0,y)/\sigma_0$; (b) For the in-plane stress $\sigma_{yy}(0,y)/\sigma_0$, where $\sigma_0 = P/2a$.

Table 4
Stress singularities β_1, β_2 and the non-dimensional stress intensity factors $F_I(a)/F_{01}$, $F_I(-a)/F_{02}$ at the contact edges for different values of μ_f, with fixed $\mu_1/\mu_3 = 0.2$, $a/h = 0.2$ and $v_0 = 0.2$.

	$\mu_f = 0.1$ $\beta_1 = -0.4909$ $\beta_2 = -0.5091$	$\mu_f = 0.3$ $\beta_1 = -0.4728$ $\beta_2 = -0.5272$	$\mu_f = 0.5$ $\beta_1 = -0.4548$ $\beta_2 = -0.5451$	$\mu_f = 0.8$ $\beta_1 = -0.4285$ $\beta_2 = -0.5715$
$F_I(a)/F_{01}$	0.2570	0.2374	0.2081	0.1408
$F_I(-a)/F_{02}$	0.2492	0.2231	0.2024	0.1868

From Fig. 7(a) and Table 5, it appears that the increase in the thermal expansion coefficient, α_1/α_3, can improve slightly the stress concentrations at both contact edges. While Fig. 7(b) indicates that the distributions of the in-plane stress hardly depends on the non-dimensional parameter α_1/α_3.

The effects of the non-dimensional thermal conductivity coefficient, k_1/k_3, on the contact stress are demonstrated in Fig. 8(a) and (b). From Fig. 8(a) and the stress intensity factors in Table 5, one can see that the increase in the thermal conductivity coefficient results in the stress concentration relieving around both contact edges. The fact that coatings with a higher thermal conductivity can facilitate the heat transfer within the coated system can be understood to explain such relaxation. From Fig 8(b), it is interesting to find that the in-plane stress substantially changes to be compressive with an increasing k_1/k_3, especially the stress behind the trailing edge. Thus, it can infer that higher thermal conductivity at the contact surface can prevent effectively the graded layer from cracking damage during sliding friction.

6.4. Surface temperature distribution under the punch

Non-dimensional surface temperature distribution Θ/Θ_0 under the sliding punch for various relative sliding speed v_0 is plotted in Fig. 9, where we define $\Theta_0 = \frac{\mu_f^* \sigma_0 k_1 (\kappa+1)}{k_* \mu_1 \alpha_1^*}$ and μ_f^* is a typical value of frictional coefficient, k_* a typical value of the thermal conductivity coefficient. In the numerical analysis, we choose $k_* = 10$ and $\mu_f^* = 0.5$. From Fig. 9, one can see that the non-dimensional surface temperature Θ/Θ_0 at the trailing side is higher than that at the leading side due to heat transfer effects. When the sliding speed vanishes, the surface temperature vanishes too. It is reasonable to find that the surface temperature increases with an increasing sliding speed v_0.

The relation between the non-dimensional surface temperature Θ/Θ_0 and the friction coefficient μ_f is shown in Fig. 10, in which one can see that the distribution of surface temperature is non-uniform in the contact area. Similar to the phenomenon in Fig. 9, the temperature is slightly higher at the trailing side than that at the leading side. Furthermore, it is found that the surface temperature tends to increase significantly with an increasing friction coefficient.

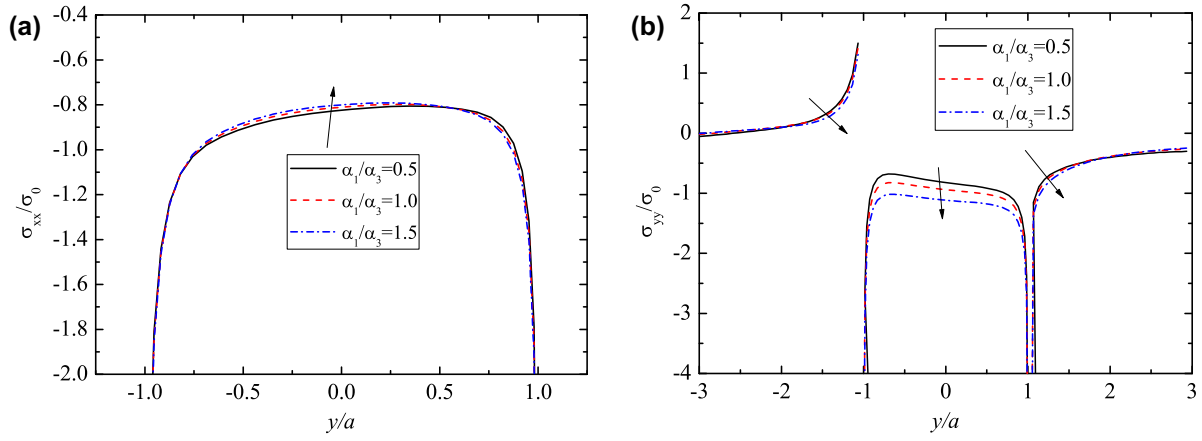

Fig. 7. Distributions of the non-dimensional contact stresses along the contact interface for different thermal expansion coefficients α_1/α_3 with fixed values $\mu_1/\mu_3 = 0.2$, $v_0 = 0.2$, $\mu_f = 0.5$, $a/h = 0.2$. (a) For the contact pressure $\sigma_{xx}(0,y)/\sigma_0$; (b) For the in-plane stress $\sigma_{yy}(0,y)/\sigma_0$, where $\sigma_0 = P/2a$.

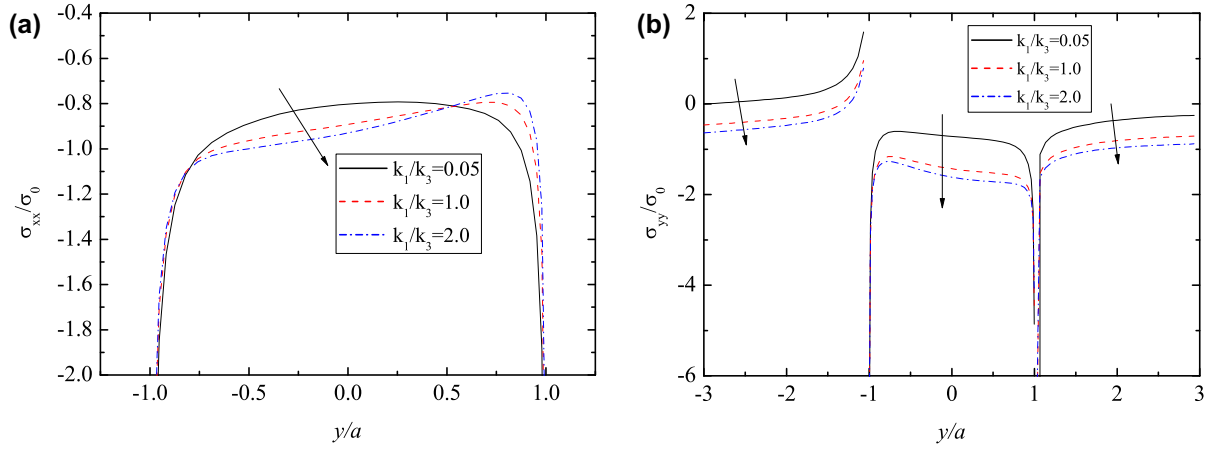

Fig. 8. Distributions of the non-dimensional contact stresses along the contact interface for different thermal conductivity ratios k_1/k_3 with fixed values $\mu_1/\mu_3 = 0.2$, $v_0 = 0.2$, $\mu_f = 0.5$, $a/h = 0.2$. (a) For the contact pressure $\sigma_{xx}(0,y)/\sigma_0$; (b) For the in-plane stress $\sigma_{yy}(0,y)/\sigma_0$, where $\sigma_0 = P/2a$.

Table 5
The non-dimensional stress intensity factors $F_I(a)/F_{01}$, $F_I(-a)/F_{02}$ at the contact edges for different values of k_1/k_3 and α_1/α_3 with fixed $\mu_1/\mu_3 = 0.2$, $a/h = 0.2$, $\mu_f = 0.5$ and $v_0 = 0.2$.

k_1/k_3	$F_I(-a)/F_{02}$	$F_I(a)/F_{01}$	α_1/α_3	$F_I(-a)/F_{02}$	$F_I(a)/F_{01}$
0.05	0.2194	0.2078	0.5	0.2072	0.2019
1.0	0.1664	0.1847	1.0	0.2170	0.2063
2.0	0.1413	0.1762	1.5	0.2246	0.2098

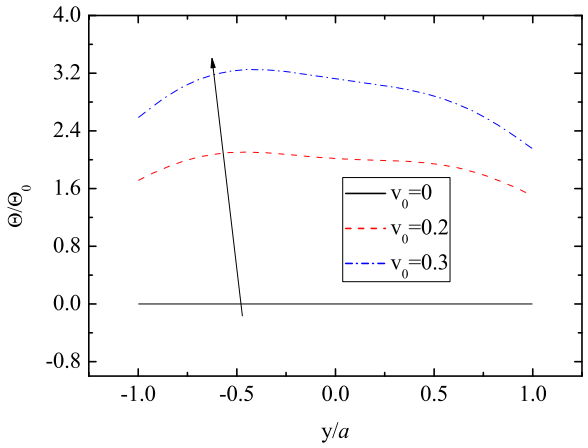

Fig. 9. Distributions of the non-dimensional temperature Θ/Θ_0 in the contact region for different nondimensional sliding speeds v_0 with fixed values $\mu_1/\mu_3 = 0.2$, $a/h = 0.2$ and $\mu_f = 0.5$, where $\Theta_0 = \frac{\mu_f^* \sigma_0 k_1 (\kappa+1)}{k_* \mu_1 \alpha_1^*}$.

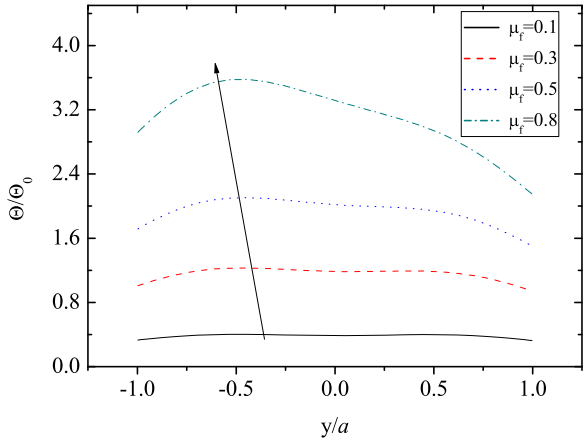

Fig. 10. Distributions of the non-dimensional temperature Θ/Θ_0 in the contact region for different frictional coefficients μ_f with fixed values $\mu_1/\mu_3 = 0.2$, $a/h = 0.2$ and $v_0 = 0.2$, where $\Theta_0 = \frac{\mu_f^* \sigma_0 k_1 (\kappa+1)}{k_* \mu_1 \alpha_1^*}$.

7. Conclusions

A thermo-mechanical contact model is investigated, in which a rigid punch slides on a finite graded layer fixed on a rigid foundation. Exponential variation law in the thickness direction is adopted for the graded layer's material property, such as the elastic modulus, thermal conductivity coefficient and the thermal expansion coefficient. The frictional heat effect is mainly focused on and compared to the corresponding isothermal contact model. It is found that the distributions of the contact stress and the in-plane surface stress are significantly influenced by the shear modulus, relative sliding speed, friction coefficient, and thermal parameters. Stress singularities and the stress intensity factors at both contact edges are obtained. In addition, the surface temperature in the contact region induced by the frictional sliding is also analyzed. Main conclusions are made as follows,

(1) Stress singularity at the trailing edge is much stronger than that at the leading edge. The in-plane normal stress is unbounded and discontinuous at both contact edges.
(2) The shear modulus ratio, μ_1/μ_3, has remarkable influences on both the contact pressure and in-plane stress. A larger μ_1/μ_3 will result in more serious stress concentration at both contact edges as well as improving in-plane tensile stress behind the trailing edge. It is reasonable to design a graded layer with a softer surface in order to prevent cracking damage induced by sliding friction.
(3) Decreasing friction coefficient, layer thickness or increasing sliding speed or thermal conductivity coefficient could decrease the in-plane tensile stress behind the trailing edge. In order to prevent the material from possible cracking and contact damage during the process of sliding contact, one can tune these parameters properly.
(4) The surface temperature at the trailing side is slightly higher than that at the leading one due to heat transfer effect. Furthermore, the surface temperature will increase significantly with either an increasing sliding speed or an increasing friction coefficient.

The results in the present paper should be helpful for the design of novel graded materials with potential applications in aerospace, tribology, thin films, coatings and other engineering fields.

Acknowledgements

The work reported here is supported by NSFC through Grants #10972220, #10732050, #11021262 and Project 2012CB937500.

References

Alblas, J.B., Kuipers, M., 1971. The two dimensional contact problem of a rough stamp sliding slowly on an elastic layer—I. General considerations and thick layer asymptotics. Int. J. Solids Struct. 7, 99–109.
Barber, J.R., 1976. Some thermoelastic contact problems involving frictional heating. Q. J. Mech. Appl. Math. 29, 1–13.
Barber, J., Comninou, M., 1989. Thermoelastic contact problems. Therm. Stresses 3, 1–106.
Barik, S.P., Kanoria, M., Chaudhuri, P.K., 2008. Steady state thermoelastic contact problem in a functionally graded material. Int. J. Eng. Sci. 46, 775–789.
Chen, S.H., Chen, P.J., 2010. Nanoadhesion of a power-law graded elastic material. Chin. Phys. Lett. 27.
Chen, S.H., Yan, C., Soh, A., 2009a. Adhesive behavior of two-dimensional power-law graded materials. Int. J. Solids Struct. 46, 3398–3404.
Chen, S.H., Yan, C., Zhang, P., Gao, H.J., 2009b. Mechanics of adhesive contact on a power-law graded elastic half-space. J. Mech. Phys. Solids 57, 1437–1448.
Choi, H.J., 2009. On the plane contact problem of a functionally graded elastic layer loaded by a frictional sliding flat punch. J. Mech. Sci. Technol. 23, 2703–2713.
Choi, H.J., Paulino, G.H., 2008. Thermoelastic contact mechanics for a flat punch sliding over a graded coating/substrate system with frictional heat generation. J. Mech. Phys. Solids 56, 1673–1692.
Choi, H.J., Paulino, G.H., 2010. Interfacial cracking in a graded coating/substrate system loaded by a frictional sliding flat punch. Proc. R. Soc. A Math. Phys. Eng. Sci. 466, 853–880.
Ciavarella, M., Barber, J.R., 2005. Stability of thermoelastic contact for a rectangular elastic block sliding against a rigid wall. Eur. J. Mech. A Solids 24, 371–376.
Conway, H.D., Vogel, S.M., Farnham, K.A., So, S., 1966. Normal and shearing contact stresses in indented strips and slabs. Int. J. Eng. Sci. 4, 343–359.
Dag, S., Erdogan, F., 2002. A surface crack in a graded medium loaded by a sliding rigid stamp. Eng. Fract. Mech. 69, 1729–1751.
El-Borgi, S., Abdelmoula, R., Keer, L., 2006. A receding contact plane problem between a functionally graded layer and a homogeneous substrate. Int. J. Solids Struct. 43, 658–674.
Elloumi, R., Kallel-Kamoun, I., El-Borgi, S., 2010. A fully coupled partial slip contact problem in a graded half-plane. Mech. Mater. 42, 417–428.
Giannakopoulos, A.E., Pallot, P., 2000. Two-dimensional contact analysis of elastic graded materials. J. Mech. Phys. Solids 48, 1597–1631.

Giannakopoulos, A.E., Suresh, S., 1997a. Indentation of solids with gradients in elastic properties.1. Point force. Int. J. Solids Struct. 34, 2357–2392.
Giannakopoulos, A.E., Suresh, S., 1997b. Indentation of solids with gradients in elastic properties.2. Axisymmetric indentors. Int. J. Solids Struct. 34, 2393–2428.
Guler, M.A., Erdogan, F., 2004. Contact mechanics of graded coatings. Int. J. Solids Struct. 41, 3865–3889.
Guler, M.A., Erdogan, F., 2006. Contact mechanics of two deformable elastic solids with graded coatings. Mech. Mater. 38, 633–647.
Guler, M.A., Erdogan, F., 2007. The frictional sliding contact problems of rigid parabolic and cylindrical stamps on graded coatings. Int. J. Mech. Sci. 49, 161–182.
Guo, X., Jin, F., Gao, H.J., 2011. Mechanics of non-slipping adhesive contact on a power-law graded elastic half-space. Int. J. Solids Struct. 48, 2565–2575.
Hills, D.A., Barber, J.R., 1985. Steady motion of an insulating rigid flat-ended punch over a thermally conducting half-plane. Wear 102, 15–22.
Hills, D.A., Barber, J.R., 1986. Steady sliding of a circular cylinder over a dissimilar thermally conducting half-plane. Int. J. Mech. Sci. 28, 613–622.
Hills, D.A., Nowell, D., Sackfield, A., 1993. Mechanics of Elastic Contacts. Butterworth-Heinemann, Oxford.
Jaffar, M.J., 2002. Frictionless contact between an elastic layer on a rigid base and a circular flat-ended punch with rounded edge or a conical punch with rounded tip. Int. J. Mech. Sci. 44, 545–560.
Jin, F., Guo, X., 2010. Non-slipping adhesive contact of a rigid cylinder on an elastic power-law graded half-space. Int. J. Solids Struct. 47, 1508–1521.
Joachim-Ajao, D., Barber, J.R., 1998. Effect of material properties in certain thermoelastic contact problems. J. Appl. Mech. Trans. ASME 65, 889–893.
Jorgensen, O., Giannakopoulos, A.E., Suresh, S., 1998. Spherical indentation of composite laminates with controlled gradients in elastic anisotropy. Int. J. Solids Struct. 35, 5097–5113.
Ke, L.L., Wang, Y.S., 2006. Two-dimensional contact mechanics of functionally graded materials with arbitrary spatial variations of material properties. Int. J. Solids Struct. 43, 5779–5798.
Ke, L.L., Wang, Y.S., 2007. Two-dimensional sliding frictional contact of functionally graded materials. Eur. J. Mech. A Solids 26, 171–188.
Ke, L.L., Wang, Y.S., 2008. Fretting contact with finite friction of a functionally graded coating with arbitrarily varying elastic modulus. Part 1: Normal loading. J. Strain Anal. Eng. Des. 43, 273–274.
Ke, L.L., Wang, Y.S., 2010. Fretting contact of two dissimilar elastic bodies with functionally graded coatings. Mech. Adv. Mater. Struct. 17, 433–447.
Krumova, M., Klingshirn, C., Haupert, F., Friedrich, K., 2001. Microhardness studies on functionally graded polymer composites. Compos. Sci. Technol. 61, 557–563.
Liu, T.J., Wang, Y.S., 2008. Axisymmetric frictionless contact problem of a functionally graded coating with exponentially varying modulus. Acta Mech. 199, 151–165.
Liu, J., Ke, L.L., Wang, Y.S., 2011. Two-dimensional thermoelastic contact problem of functionally graded materials involving frictional heating. Int. J. Solids Struct. 48, 2536–2548.
Pauk, V., 1994. Plane contact problem involving heat generation and radiation. J. Theor. Appl. Mech. 32, 829–839.
Pauk, V.J., 1999. Plane contact problem for a layer involving frictional heating. Int. J. Heat Mass Transfer 42, 2583–2589.
Pauk, V.J., Wozniak, C., 1999. Plane contact problem for a half-space with boundary imperfections. Int. J. Solids Struct. 36, 3569–3579.
Pauk, V., Wozniak, M., 2003. Frictional heating effects in the plane contact of layer and rigid flat punch. J. Tech. phys. 44, 237–244.
Pender, D.C., Padture, N.P., Giannakopoulos, A.E., Suresh, S., 2001a. Gradients in elastic modulus for improved contact-damage resistance. Part I: The silicon nitride–oxynitride glass system. Acta Mater. 49, 3255–3262.
Pender, D.C., Thompson, S.C., Padture, N.P., Giannakopoulos, A.E., Suresh, S., 2001b. Gradients in elastic modulus for improved contact-damage resistance. Part II: The silicon nitride–silicon carbide system. Acta Mater. 49, 3263–3268.
Reina, S., Dini, D., Hills, D.A., 2010. Interfacial slip and creep in rolling contact incorporating a cylinder with an elastic layer. Eur. J. Mech. A Solids 29, 761–771.
Rhimi, M., El-Borgi, S., Ben Said, W., Ben Jemaa, F., 2009. A receding contact axisymmetric problem between a functionally graded layer and a homogeneous substrate. Int. J. Solids Struct. 46, 3633–3642.
Suresh, S., 2001. Graded materials for resistance to contact deformation and damage. Science 292, 2447–2451.
Suresh, S., Mortensen, A., 1998. Fundamentals of functionally graded materials: processing and thermomechanical behaviour of graded metals and metal-ceramic composites. Book Inst. Mater. 698.
Suresh, S., Giannakopoulos, A.E., Alcala, J., 1997a. Spherical indentation of compositionally graded materials: theory and experiments. Acta Mater. 45, 1307–1321.
Suresh, S., Giannakopoulos, A.E., Alcala, J., 1997b. Spherical indentation of compositionally graded materials: theory and experiments. Acta Mater. 45, 3087–3087.
Suresh, S., Olsson, M., Giannakopoulos, A.E., Padture, N.P., Jitcharoen, J., 1999. Engineering the resistance to sliding-contact damage through controlled gradients in elastic properties at contact surfaces. Acta Mater. 47, 3915–3926.
Yevtushenko, A.A., Kulchytskyzhyhailo, R.D., 1995. Determination of limiting radii of the contact area in axismmetrical contact problems with frictional heat-generation. J. Mech. Phys. Solids 43, 599–604.
Zhou, Y.T., Lee, K.Y., 2011. Thermo-electro-mechanical contact behavior of a finite piezoelectric layer under a sliding punch with frictional heat generation. J. Mech. Phys. Solids 59, 1037–1061.